Peer-reviewed version available at *Int. J. Mol. Sci.* **2019**, *20*, 2580; doi:10.3390/ijms20102580

Article

Knockdown of NANOG reduces cell proliferation and induces G0/G1 cell cycle arrest in human Adipose Stem Cells

Maria Pitrone[1], Giuseppe Pizzolanti[13]*, Antonina Coppola[1], Laura Tomasello[1], Stefania Martorana[2], Gianni Pantuso[2] and Carla Giordano [13]*

1 Aldo Galluzzo Laboratory of Regenerative Medicine, Department of Health Promotion Sciences, Maternal and infant Care, Internal Medicine and Medical Specialties, PROMISE, University of Palermo, Italy; maria.pitrone@unipa.it (M.P.); laura.tomasello@unipa.it (L.T.); antonina.coppola02@unipa.it (A.C.);
2 Department of Surgical, Oncological and Oral Sciences, Division of General and Oncological Surgery, University of Palermo, Palermo, Italy. stefania.martorana@unipa.it (S.M.); gianni.pantuso@unipa.it (G.P.)
3 ATeN (Advanced Technologies Network Center), University of Palermo, 90127 Palermo, Italy
* Correspondences: giuseppe.pizzolanti@unipa.it (G.P.); carla.giordano@unipa.it (C.G.); Tel.: +39-091-6552138 (G.P.); +39-091-6552110 (C.G.); Fax: +39-091-6552138 (G.P.); +39-091-6552123 (C.G.)

Abstract: The core components of regenerative medicine are stem cells with high self-renewal and tissue regeneration potentials. Adult stem cells can be obtained from many organs and tissues. NANOG, SOX2 and OCT4 represent the core regulatory network that suppresses differentiation-associated genes, maintaining the pluripotency of mesenchymal stem cells. The roles of NANOG in maintaining self-renewal and undifferentiated status of adult stem cells are still not perfectly established. In this study we define the effects of downregulation of NANOG in maintaining self-renewal and undifferentiated state in mesenchymal stem cells (MSCs) derived from subcutaneous adipose tissue (hASCs). hASCs were expanded and transfected in vitro with short hairpin Lentivirus targeting NANOG. Gene suppressions were achieved at both transcript and proteome levels. The effect of NANOG knockdown on proliferation after 10 passages and on the cell cycle was evaluated by proliferation assay, colony forming unit (CFU), qRT-PCR and cell cycle analysis by flow-cytometry. Moreover, NANOG involvement in differentiation ability was evaluated. We report that downregulation of NANOG revealed a decrease in the proliferation and differentiation rate, inducing cell cycle arrest by increasing p27/CDKN1B (Cyclin-dependent kinase inhibitor 1B) and p21/CDKN1A(Cyclin-dependent kinase inhibitor 1A) through p53 and regulate DLK1/PREF1. Furthermore, NANOG induced downregulation of DNMT1, a major DNA methyltransferase responsible for maintaining methylation status during DNA replication probably involved in cell cycle regulation. Our study confirms that NANOG regulates the complex transcription network of plasticity of the cells, inducing cell cycle arrest and reducing differentiation potential.

Keywords: Human adipose stem cell; NANOG; Cell cycle regulation; DNMT1; Lentiviral transduction;

1. Introduction

OCT4, SOX2 and NANOG together form the core regulatory network that suppresses differentiation-associated genes , maintaining the pluripotency of cells [1]. Expression of OCT4 and NANOG is restricted to pluripotent cells, and they are downregulated upon differentiation [2,3]. OCT4 and NANOG work together to maintain pluripotency in the absence of feeder layer or extrinsic factor LIF [4] while downregulation of NANOG induces ESC differentiation into extraembryonic lineages [5,6]. Although OCT4 and NANOG are known to maintain self-renewal and block differentiation in ESCs [7], little is still known about their mechanism in adult mesenchymal stem cells. Adipose stem cells (ASC) represent an alternative source of mesenchymal stem cells that can be easily and safely obtained from adipose tissue, growing under appropriate culture conditions for a long time [8–10]. ASCs are characterized by a well-defined cell-surface antigen phenotype consisting of both expression of antigens such as CD29, CD90, CD105 and CD73 and the absence of hematopoietic-endothelial markers such as CD34, CD45, CD117, and HLA-DR [11–14]. There is still great interest in better understanding the mechanisms underlying the proliferation, differentiation, and heterogeneity of these cells [15,16]. OCT4, SOX2, and NANOG have also been suggested to play a similar role as embryonic stem cells in adult mesenchymal cells, including human Adipose Stem Cells (hASCs). In our previous studies we found that the embryonic stem cell marker NANOG is over-expressed in MSCs derived from adipose tissue and its silencing with a RNA interference technology causes downregulation of OCT4 and SOX2 gene expression [13], confirming recent studies that have demonstrated a central role of NANOG in regulating stem cells' multipotent properties [15,17].

DLK1(PREF1) is a marker used to characterized mouse preadipocyte progenitors which inhibits adipogenesis, suppressing C/EBPβ and C/EBPδ gene expression [18–23]. Recently, DLK1(PREF1) proved to be a useful marker for human ASC [24,25] and methylation regulates its expression. DNMT1 is a major DNA methyltransferase responsible for maintaining methylation status during DNA replication [25]. DNA methylation seems to play an essential role in regulating ESC differentiation and embryo development. A recent study [26] demonstrated that NANOG directly binds to the promoter of DNMT1 [26] and enhances its expression. In this study our aim was to investigate the role of NANOG in maintaining the proliferation and differentiation potential of ASCs after downregulation of NANOG with a Lentivirus system and to examine the expression of some important genes related to cell growth control such as p27/CDKN1B, p21/CDKN1A, CCDN1 and PREF1. We show that *NANOG* downregulation induced a decrease in the proliferation rate and differentiation potential and led to cell cycle arrest in G0/G1 by regulating *CCDN1*, *p21/CDKN1A* and *p27/CDKN1B* through *p53* and a *PREF1* inhibition, inducing loss of pluripotency via *DNMT1*.

2. Results

2.1. hASC isolation and characterization

Enzymatic digestion of biopsied human adipose tissue was obtained after consent from 20 patients (9 men and 11 women; age 45±10 years; with body mass index (BMI) range 28 ± 3) undergoing elective open-abdominal surgery. As previously published, hASC highly expressed *THY1*, *CD105* and *CD73* and all of the ESC markers *SOX-2*, *OCT4* and *NANOG* (see Table S1 in supplementary). When cultured in adhesion we observed the formation of colonies of fibroblastic-like cells, whereas in low-adhesion culture conditions spheres were formed (Fig. 1).

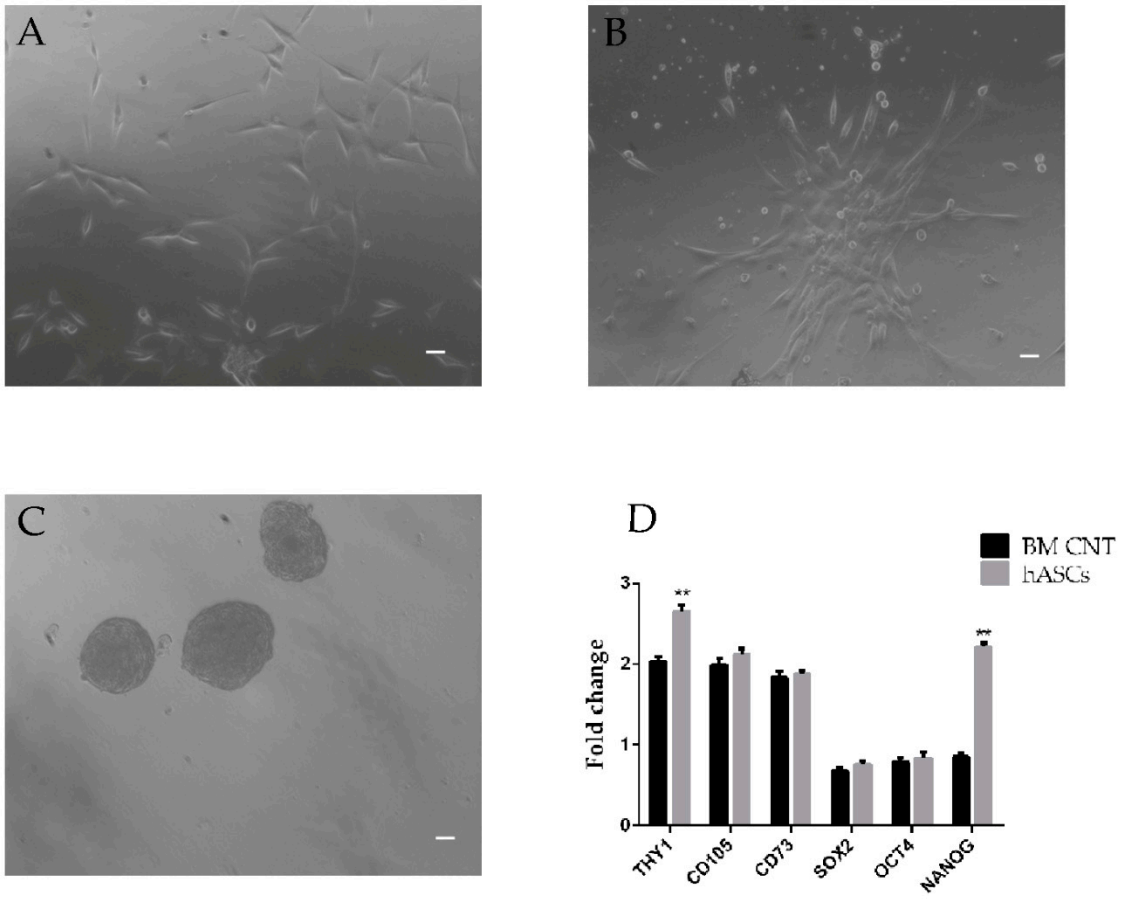

Figure. 1 hASC morphology on day 5 (A) of expansion culture observed under light microscopy (10x) with phase contrast with a Nikon DS-FI1 CCD camera. B shows the formation of colonies when cultured in adhesion while C shows spheres which formed when cells were cultured in low adhesion culture conditions. A representative experiment referring to 23 samples studied. (D) qRT-PCR analysis in freshly isolated hASCs at passage 4 of *THY1*, *CD73*, *CD105*, *OCT4*, *SOX2* and *NANOG* gene expression. Relative expression levels were assessed using the $2^{-\Delta\Delta Ct}$ method. Values are shown as mean ± SE, **p<0.01. Data shown are relative to an endogenous control (beta-Actin), with fold change compared to expression levels of Bone Marrow mesenchymal stem cells commercially acquired. Data are representative of three independent experiments.

1.2. Knockdown of *NANOG* silencing by lentivirus.

To determine the roles of NANOG in maintaining stem cell properties we evaluated changes in stem cell marker gene expression in hASC lentiviral transducted with shRNAs against NANOG. The mRNA and protein expression level of *NANOG* after 10 and 15 days of antibiotic selection after shRNA infection was evaluated by quantitative PCR and western blot analysis. As observed in Fig. 2A , the *NANOG* mRNA level decreased by almost 90% ± 3.5% in cell lines infected with NANOG shRNA lentivirus as compared to the NC group. Furthermore, Fig. 2B showed the downregulation of NANOG protein expression after 15- day antibiotic selection, by almost 76% ± 2.3% in hASCs infected with NANOG shRNA lentivirus (Optical Density (OD)= 0.87 ± 0.9 vs. 0.2 ± 0.06). The quantitative analysis of western blot bands was performed using ImageJ. In our previous studies we found that the embryonic stem cell marker NANOG is over-expressed in hASCs and its silencing causes downregulation of the *OCT4* and *SOX2* genes. As assessed by real-time RT-PCR, we confirm that NANOG mRNA in freshly hASC is highly expressed and NANOG knockdown

induced *OCT4* and *SOX2* downregulation, indicating loss of pluripotency in hASC (data shown in supplementary materials).

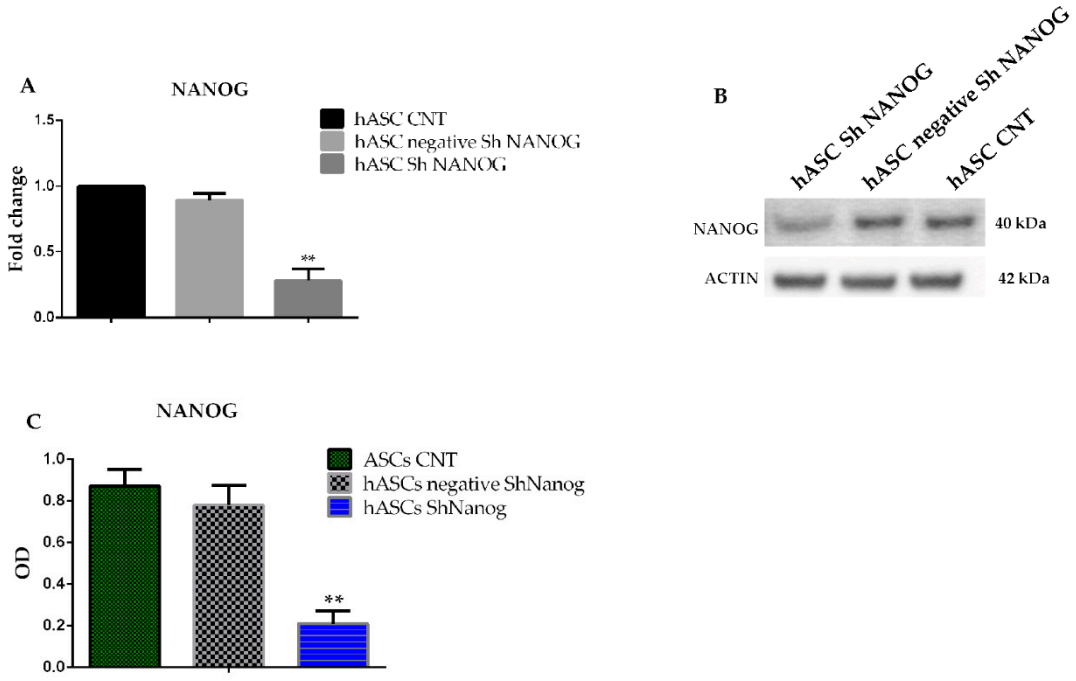

Figure. 2 hASCs lentivirally transducted with scrambled (negative) or ShRNA against NANOG. (A) qRT-PCR analysis for *NANOG* gene expression after 10-day antibiotic selection. Relative expression levels were assessed using the $2^{-\Delta\Delta Ct}$ method. Data are representative of three independent experiments with the fold change compared to expression levels in a commercial human adipose stem cell line (ASC52telo, hTERT immortalized adipose-derived mesenchymal stem cells). Values shown as the mean ± SE, **p<0.01. (B and C) Western blot analysis for protein expression of NANOG after 15 days of antibiotic selection. Values are shown as mean ± SE,**p<0.01.

2.2. Analysis of PREF1

To better understand the differentiation potential of hASCs biology we studied the effect of NANOG shRNA knockdown on the *DLK1/PREF1* gene expression. We found that *PREF1* mRNA was downregulated (0.8 ± 0.03 vs. 0.3 ± 0.06, p<0.01) in hASC with *NANOG* downregulated.

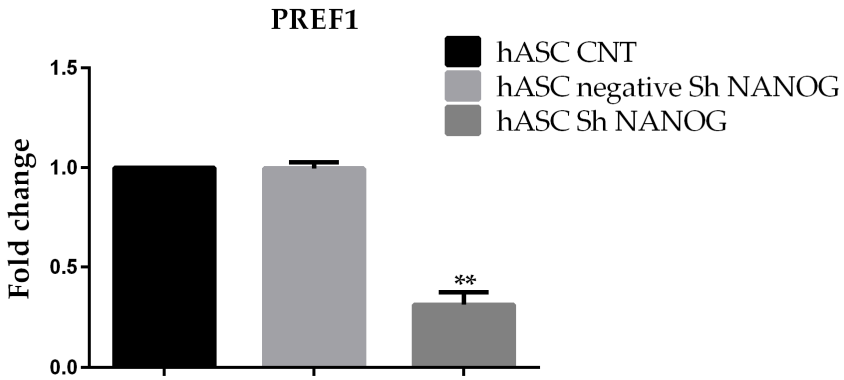

Figure. 3 qRT-PCR analysis showed the expression of *PREF1* was significantly downregulated following inhibition of NANOG in hASC. Relative expression levels were assessed using the 2-ΔΔCt method. Data are representative of three independent experiments with the fold change compared to expression levels in a commercial human adipose stem cell line (ASC52telo, hTERT immortalized adipose-derived mesenchymal stem cell). The experiment was repeated at least three times **p<0.01

2.3. Downregulation of *NANOG* inhibited cell proliferation, increased population doubling time and reduced differentiation potential.

The effects of *NANOG* knockdown on ASC proliferation were assessed using trypan blue assay and Colony Forming Unit ability. Analysis of cell proliferation indicated that the hASCs expressing NANOG shRNA grew significantly more slowly than wild-type cells and control cells, and this difference became more evident after 3 days (Fig. 4A). Quantitative analysis of colonies revealed that after incubation for 14 days, the number of colonies of NANOG shRNAs-infected cells was lower than that of the parent and control cells. As shown in Fig.4B the clonogenicity of ASCs transfected with sh lentivirus NANOG decreased, according to the number of cell colonies. The colony formation rate of NANOG shRNAs-infected cells was 8.5±3.6%, lower than that of non-transfected and control shNANOG tranfected cells (**p<0.01) and the results show an increase in the population doubling time (Fig.4C). ASCs with NANOG knockdown also shows a decrease in adipogenic differentiation potential (Figure 4D). Taken together, hASCs with NANOG knockdown decreased proliferation capacity and differentiation potential, indicating the functional role of NANOG in regulation of the stem cell properties of hASCs.

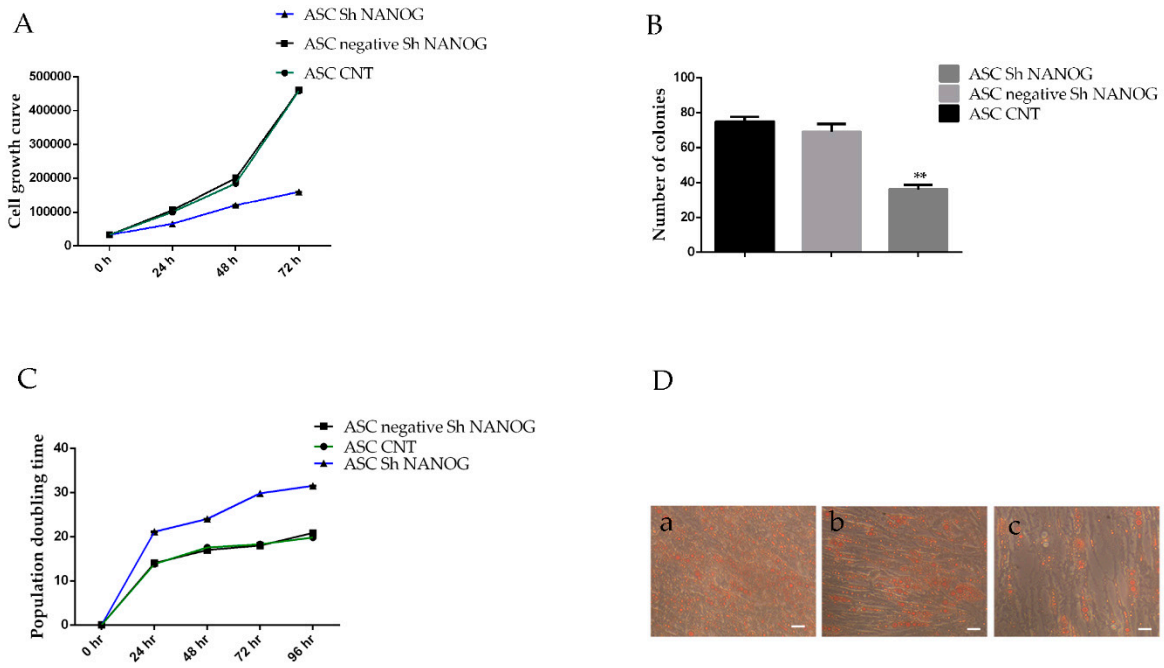

Figure. 4 Time-dependent effects of downregulation of NANOG on hASC growth, colony formation ability, population doubling time and differentiation potential. A shows the cell growth rate over a 72-hr period in hASCs lentivirally transduced with scrambled (negative NANOG) or shRNAs against NANOG using the trypan blue viability assay. (B) The clone numbers (more than 50 cells) of the hASC control (ASC CNT) and hASC negative Sh NANOG were much higher than that of the hASC Sh NANOG (75 ± 5 vs. 40 ± 5). (C) The population doubling time analysis. D shows the differentiation potential into adipogenic lineage. Cultures were observed under light microscopy (10x) with phase contrast with a Nikon DS-FI1 CCD camera. (Values are mean ± SD,

**p<0.01). A representative photograph of the colonies formed 14 days after lentivirus transfection, stained with crystal violet, are shown in supplementary materials.

2.4. Knockdown of NANOG inhibited the expression of *CCND1/Cycline D1*, enhanced the expression of *p21* and *p27* and induced cell cycle block in the G0/G1 phase

To evaluate the effects of NANOG knockdown on the growth capability of ASCs, we examined cell cycle distributions in NANOG knockdown cells and control cells. The percentage of cells in G0/G1 phase increased from 48% ± 3.2% for hASC controls and 52% ± 1.8% for negative shRNA controls to 70.5± % (NANOG knockdown group), while the percentage of S phase cells decreased from 45% ± 2.3% for hASC controls and 48% for negative shRNA controls to 20% (NANOG knockdown group). (Fig.5 A) These results indicated that downregulation of NANOG expression arrested hASCs in the G0/G1 phase. Consistently with these observations downregulation of NANOG induced a reduction of the proliferation rate as indicated by the proliferation index (P.I.) 0.52% ± 0.06 in hASC negative for ShRNA against NANOG vs. P.I 0.23 ± 0.001 in hASCs transfected with ShRNAs against NANOG . To investigate the G0/G1 phase arrest we evaluated the principal genes involved in cell proliferation, *p27/CDKN1B* (Cyclin-dependent kinase inhibitor 1B) *p21/CDKN1A*(Cyclin-dependent kinase inhibitor 1A) and *CYCLINE D1* by qRT-PCR. Interestingly, as shown in Fig. 5, knockdown of *NANOG* in hASCs increased expression of the *CDKN1B* and *CDKN1A* (1.8 ± 0.08-fc and 3.8±0.05-fc respectively **p<0.01) mRNA level when compared to the negative ShNANOG and control cells (0.85±0.05). Significant downexpression of *CYCLINE D1* in mRNA levels was detected (0.63 ± 0.09-fc, ** p<0.01).

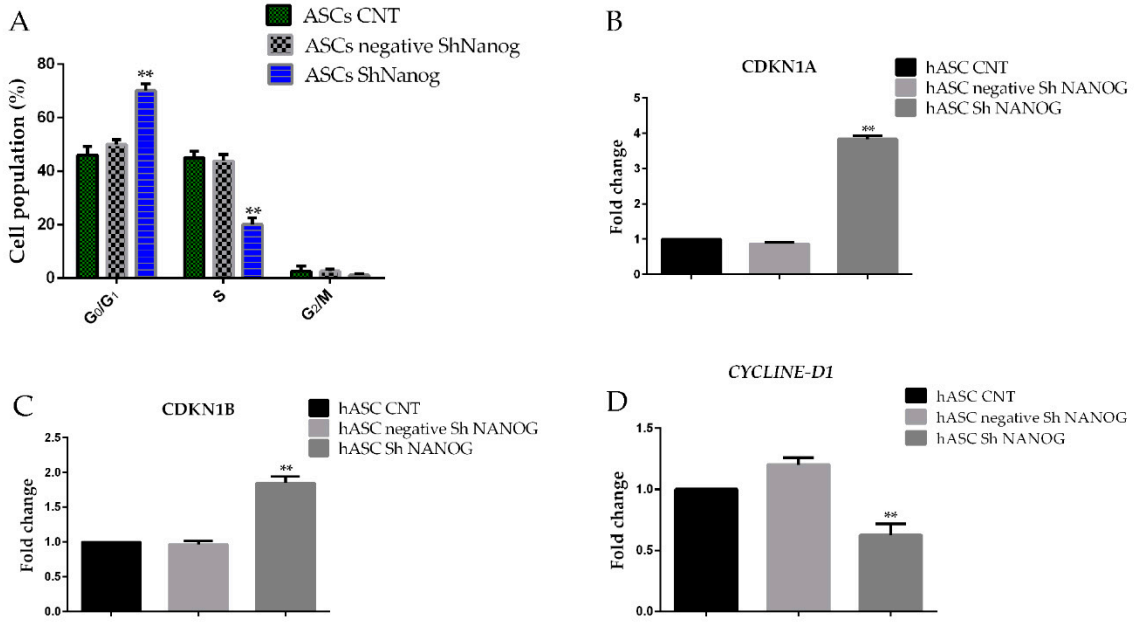

Figure 5. Changes in hASC cell cycle distribution as a result of *NANOG* downregulation. A shows cell cycle distribution of hASCs according to Nicoletti's protocol. (B) Real-time PCR analyses showed that expression of the cell cycle protein *CDKN1B* was significantly increased while the expression of *CYCLINE D1* was downregulated (B). Flow cytometry analyses showed that downregulation of NANOG induced a decrease in the proportion of G2/M + S phase cells in hASC cells as compared to controls. All experiments were repeated at least three times.

2.5. Knockdown of NANOG regulates DNMT1

To know the role of *p53* in regulation of *p21* and *p27* gene expression in hASC with *NANOG* downregulated we evaluated *p53* mRNA expression. Our findings confirmed that hASCs expressed

p53 and *NANOG* downregulation induced a significant change in *p53* (0.5 ± 0.08-fc *p<0.05) gene expression, as shown in figure 6A. DNA methylation seems to play an essential role in regulating ESC differentiation and embryo development and Dnmts-mediated CpG methylation has been demonstrated to play a distinct role in cell cycle regulation. To investigate the possible involvement of DNMTs in cell cycle arrest we evaluated expression of the DNMT1 protein in hASC lentivirally transduced with shRNA targeting NANOG. We found that DNMT1 protein level were dramatically reduced in hASC with NANOG knockdown compared to control cells (optical density (OD)= 0.2 ± 0.03 vs. 0.4 ± 0.06). (Figure 6B and 6C)

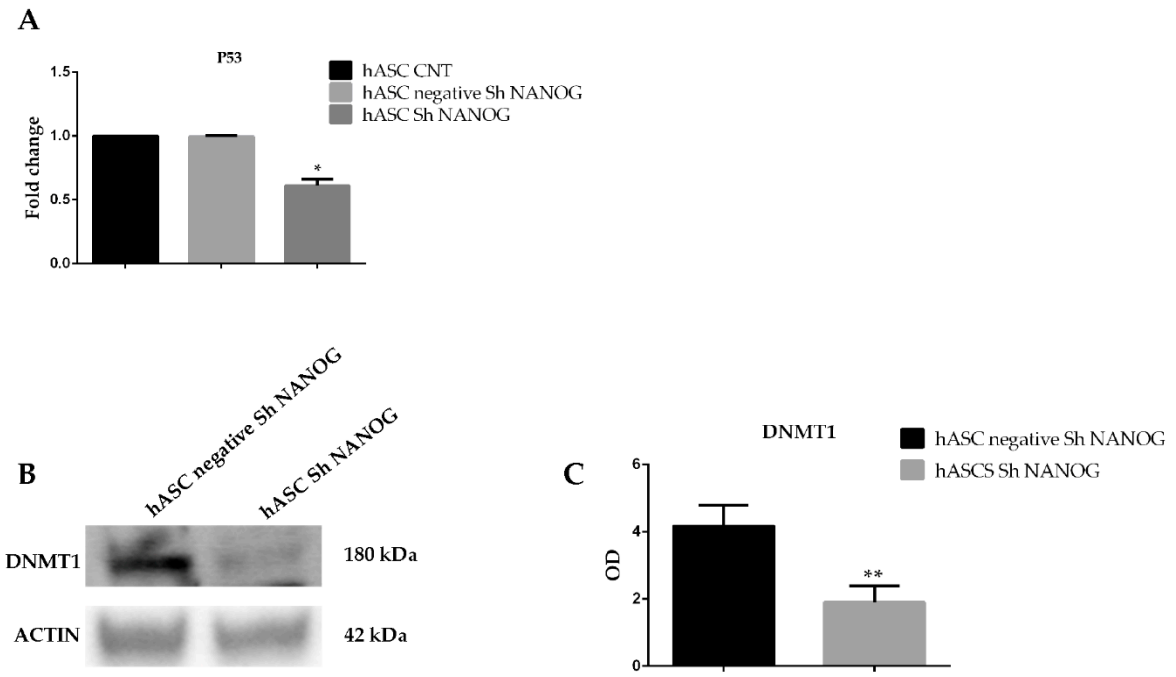

Figure 6.(A) qRT-PCR analysis showed that expression of *p53* was significantly downregulated following inhibition of NANOG in hASC. Relative expression levels were assessed using the $2^{-\Delta\Delta Ct}$ method. Data are representative of three independent experiments with the fold change compared to expression levels in a commercial human adipose stem cell line (ASC52telo, hTERT immortalized adipose-derived mesenchymal stem cell). The experiment was repeated at least three times *p<0.05. (B) Representative western blot analysis for expression of DNMT1. Densitometric analysis of the Western blot depicted in (C). The histograms are the results of three independent experiments. The values are shown as the mean ± SE, ** p < 0.01. OD, optical density (** p < 0.01).

3. Discussion

The ability to proliferate and to retain an undifferentiated state, such as the capability to differentiate toward multiple cell lineages, is a property of stem cells. It is well known that SOX2 OCT4 and NANOG are the core of "pluripotency" machinery. Our previous study suggested that *NANOG* is an essential transcriptional regulator of genes involved in maintaining the undifferentiated pluripotent state of hASCs, but few data exist to conclude that the hASC fate and differentiation potential are regulated by this protein. In this study hASCs were isolated from biopsies of subcutaneous adipose tissue undergoing elective open-abdominal surgery and were characterized for stem cell markers *CD90*, *CD105* and *CD73*, and then cells were transducted with short hairpin Lentivirus system targeting NANOG, which resulted in significant downregulation of NANOG gene and protein expression. Inhibition of *NANOG* led to a significant downregulation of *OCT4* and *SOX2*, as previously demonstrated [13], and we were able to detect a decrease in

expression of the adipose stem cell marker *DLK/PREF1*. Knockdown of NANOG in hASCs reduced cell proliferation rate and differentiation potential, inducing cell cycle arrest in G0/G1. p21 /CDKN1A and p27/ CDKN1B are proteins of the Cip/Kip family that act as key cell cycle regulators by inhibiting CDK [27,28]. To understand the roles of NANOG in cell cycle arrest we examined *p21* and *p27* gene expression. We demonstrate that downregulation of *NANOG* in hASCs induced an increase of *p27* and *p21* gene expression. Recent studies have identified CDK1 as an essential in vivo target of p27 [29] and our in vitro study confirms that *CCND1* gene expression is reduced. Moreover, we found that knockdown of NANOG led to a decrease in adipogenic differentiation potential, indicating the functional role of NANOG in regulation of stem cell properties.

It is well known that *p21* and *p27* expression is regulated largely at the transcriptional level by a *p53*-dependent mechanism [30], which suggests that NANOG may regulate expression of these "player" genes through the p53 tumor suppressor gene. Our experiments confirmed that NANOG downregulation induced a reduction of *p53* gene expression, suggesting that NANOG can regulate p21 and p27 activity through p53 activity. Furthermore, it is well known that *p21* and *p27* are regulated by methylation [31,32] and previous studies have shown that DNA methylation represents a unique epigenetic program that complements other regulatory mechanisms to ensure expression of appropriate genes in ESCs [31]. Previous experiments have shown in methylation-deficient mouse embryos (Dnmt1$^{-/-}$, Dnmt3a$^{-/-}$, and Dnmt3b$^{-/-}$) that the restoring of DNA methylation is essential for development [31–33]. One of the most important DNA methyltransferases is DNMT1, which is responsible for maintaining methylation status during DNA replication, and a recent study demonstrated that NANOG directly binds to the promoter of *DNMT1* in ESCs and enhances its expression [26]. To determine whether NANOG-mediated maintenance of stem cell properties in hASC came about through regulation of DNMT1, we evaluated DNMT1 protein expression. The results confirm that NANOG downregulation induced a reduction of DNMT1 protein expression. In conclusion, our results demonstrate that inhibition of NANOG not only decreased hASC growth and induced the arrest of the cell cycle, but also induced a reduction of differentiation ability. Moreover, our results confirm that the stem cell transcription factor NANOG regulated cell cycle progression probably via p53, which directly controls p21 and p27, key regulator factors of cell cycle machinery. Furthermore, through DNMT1 NANOG can methylate *PREF1*, which induces differentiation and can modulate the methylation status of p21 and p27 as previously described. All these data suggest that NANOG is essential for maintaining hASC properties.

4. Materials and Methods

4.1. Cell Culture and cell infection with lentiviral particles

Subcutaneous (SAT) adipose tissue biopsies were obtained from 23 consenting patients (10 men, 13 women; age 40±10; BMI range between 28±3) undergoing elective open-abdominal and laparoscopy surgery. The protocol was approved by the Independent Ethical Committee (no. 08/2018) at the Azienda Ospedaliera Universitaria Policlinico P. Giaccone, Palermo, Italy. All patients gave their written informed consent. Adipose tissue was processed as previously described [13]. Cells were used at an early passage for all experiments. For lentivirus infection, 2x10^4 hASCs were seeded in 6-well plates, and infected with lentivirus (Santa Cruz Biotechnology sc-43958-V) with a the multiplicity of infection (MOI) 10 in the presence of 8 μg/mL polybrene (Santa Cruz Biotechnology sc-134220). At 24 h after infection, the media were removed and replaced with fresh growth media. After 48h the media were replaced with fresh growth media containing puromycin (1 μg/mL Sigma Aldrich cod. P9620) to select for infected cells. All experiments were performed 10-15 days after puromycin selection.

4.2. RNA Isolation and Quantitative RT-PCR

mRNA from ASCs populations isolated from subcutaneous biopsies were isolated using an RNeasy kit (Qiagen, Hamburg, Germany) as previously described [13]. For each gene, mRNA expression

Preprints (www.preprints.org) | NOT PEER-REVIEWED | Posted: 24 April 2019 doi:10.20944/preprints201904.0264.v1

Peer-reviewed version available at Int. J. Mol. Sci. 2019, 20, 2580; doi:10.3390/ijms20102580

was normalized for the housekeeping gene beta-actin (Invitrogen). Amplification of specific transcripts was confirmed by melting curve profiles at the end of each PCR. PCR primers (Table 1) were purchased from Qiagen (QuantiTect® Primer Assays, Qiagen). All reactions were performed using the Quantitect SYBR Green PCR Kit (Qiagen cod. 204243) on the RotorGene Q Instrument (Qiagen) as previously described. Gene expression of primary cells was compared with bone marrow mesenchymal stem cells (Poietics™ Normal Human Bone Marrow Derived Mesenchymal Stem Cells Lonza PT-2501) and with a commercial primary cell line immortalized with a human telomerase reverse transcriptase (ASC52telo, hTERT) (ATCC® SCRC-4000™, American Type Culture Collection, Manassas, VA, USA), as positive cell controls. Relative expression levels for each gene were assessed using the $2^{-\Delta\Delta Ct}$ method. The results were represented as histograms with GraphPad Prism 6 Software (GraphPad Software, Inc. La Jolla, CA, USA). The qRT-PCR analyses for the stem gene were also performed after lentivirus infection experiments.

Table 1. Real-time quantitative PCR primers used for gene expression investigation

RNA	PRIMER SEQUENCES	CODE NUMBER
NANOG	Qiagen®	QT01844808
OCT3/4	Qiagen®	QT00210840
SOX2	Qiagen®	QT00237601
THY1	Qiagen®	QT00023569
CD105	Qiagen®	QT00013335
CD73	Qiagen®	QT00027279
P53	Qiagen®	QT00060235
CCDN1	Qiagen®	QT00495285
CDKN1A	Qiagen®	QT00062090
CDKN1B	Qiagen®	QT00998445
β-Actin	FORWARD: 5′-GGACTT CGA GCA AGA GAT GG-3′ REVERSE: 5′-AGC ACT GTG TTG GCG TAC AG-3′	Invitrogen

4.3.Western Blot Analysis

Proteins were extracted from adherent cultured cells and separated as previously described [13,34,35]. The antibodies used are as described in Table 2. The secondary antibody was goat anti-mouse IgG-HRP (Amersham, GE Healthcare Europe GmbH, Milan, Italy cod.). Antigen-antibody complexes were visualized using the ECL prime (Amersham, GE Healthcare Europe GmbH, Milan, Italy) on a CCD camera (Chemidoc, Bio-Rad, Milan, Italy). Western blot bands were quantified with ImageJ 1.48 software (National Institutes of Health, Bethesda, MD, USA) and the results were represented as histograms with GraphPad Prism 6 Software (GraphPad Software, Inc. La Jolla, CA, USA)

Preprints (www.preprints.org) | NOT PEER-REVIEWED | Posted: 24 April 2019 doi:10.20944/preprints201904.0264.v1

Peer-reviewed version available at Int. J. Mol. Sci. 2019, 20, 2580; doi:10.3390/ijms20102580

Table 2. Primary antibodies used

Primary Antibody/Localization Marker	**Code Number**	**Diluition**	**Incubation**
NANOG, nuclear and cytoplasmatic	sc-293121, Santa Cruz Biotechnology	1:500	o/n, 4 °C
DNMT1, nuclear	Sc-271729, Santa Cruz Biotechnology	1:500	o/n, 4 °C
B-Actin clone AC-74	A5316 Sigma Aldrich	1:10000	o/n, 4°C

4.4. Analysis of Cell Cycle Status of MSCs with lentivirus

Single-cell suspensions of control samples and transfected samples were obtained and seeded at a density of 2* 10^3 cells/cm2 (passage 3), and the DNA content was assessed according to Nicoletti's protocol [36] as previously described [13]. Data were acquired with CellQuest Pro software (Becton Dickinson), and the percentages of G1, S and G2 phase cells were calculated with the MODFIT-LT 5.0 software program (Verity Software House Inc., Topsham, ME, USA).

4.5. Colony-forming assay

Single-cell suspension ASCs cell lines were seeded in a six-well culture in DMEM/Ham's F12 1:1 supplemented with 100 units/mL penicillin, 0.1 mg/mL streptomycin and 10% fetal calf serum (FCS) at a density of 300 cells/well and cultured at 37 °C in 5% CO2. After 14 days, the cells were fixed in 4% paraformaldehyde(Sigma Aldrich) and stained with 0.1% crystal violet (Sigma Aldrich). Only the cell groups containing more than 50 cells were considered as colonies. Number of colonies were quantified with ImageJ 1.48 software (National Institutes of Health, Bethesda, MD, USA)

4.6. Population doubling and cell proliferation curve

Proliferation was assayed using trypan blue (Sigma-Aldrich) according to the manufacturer's instructions. ASCs were seeded at a density of 4×10^3 cells/cm^2 in a 96-well plate at a density of $4 \times *10^3$ cells/cm^2 and cultured up to 72 h. The cell counts were performed by optical microscope observation after trypan blue staining every 24 h during the incubation period. The doubling time (DT) was calculated in accordance with the literature data (http://www.doubling-time.com/compute.php). Three sets of experiments for each sample were used for calculations.

5. Conclusions

We examined whether NANOG contributes to maintaining cells in an undifferentiated, pluripotent state by activating certain key genes and by silencing others. For this purpose hASCs were transfected with a lentivirus with shRNAs targeting NANOG and our results suggest that NANOG plays a key role in the hASC proliferation rate by increasing the expression of p21 and p27 and by modulating PREF1. In conclusion, we confirm that NANOG is an important player in the complex transcription network that regulates pluripotency. We hypothesized that p21, p27 and PREF1 may be regulated by DNMT1, a promotor which is directly bound by NANOG, as demonstrated by Chih-Chien Tsai et al. [26]. Further experiments are needed to establish the pathway to explain the involvement of NANOG in the control of cell cycle progression.

Supplementary Materials: Supplementary materials can be found online.

Author Contributions: Maria Pitrone was responsible for the conception of the work and the design, collection and assembly of data, data analysis and interpretation and manuscript writing. Giuseppe Pizzolanti was responsible for acquisition of data and revision of the manuscript. Stefania Martorana and Gianni Pantuso were responsible for provision of biopsies . Maria Pitrone, Giuseppe Pizzolanti, Laura Tomasello and Antonina Coppola were responsible for data analysis and interpretation and drafting of the manuscript. Carla Giordano was responsible for the conception of the work and the design, data analysis and interpretation, manuscript writing and final approval of the manuscript, manuscript drafting, and critically revision for important intellectual content and financial support. All authors agree to be accountable for all aspects of the work in ensuring that questions related to the accuracy or integrity of any part of the work are appropriately investigated and resolved. All authors read and approved the final manuscript.

Funding: None

Acknowledgments: This work is dedicated to our laboratory staff.

Conflicts of Interest: The authors declare no conflict of interest

Abbreviations
Mesenchymal Stem Cell (MSC)
human Adipose Stem Cell (hASC);
p21/CDKN1A Cyclin-dependent kinase inhibitor 1A
p27/CDKN1B Cyclin-dependent kinase inhibitor 1B

1. Boyer, L. a; Boyer, L. a; Lee, T.I.; Lee, T.I.; Cole, M.F.; Cole, M.F.; Johnstone, S.E.; Johnstone, S.E.; Levine, S.S.; Levine, S.S.; et al. Core transcriptional regulatory circuitry in human embryonic stem cells. *Cell* **2005**.
2. Pan, G.; Thomson, J.A. Nanog and transcriptional networks in embryonic stem cell pluripotency. *Cell Res.* **2007**, *17*, 42–49.
3. Kim, J.; Chu, J.; Shen, X.; Wang, J.; Orkin, S.H. An Extended Transcriptional Network for Pluripotency of Embryonic Stem Cells. *Cell* **2008**.
4. Darr, H. Overexpression of NANOG in human ES cells enables feeder-free growth while inducing primitive ectoderm features. *Development* **2006**.
5. Hough, S.R.; Clements, I.; Welch, P.J.; Wiederholt, K.A. Differentiation of Mouse Embryonic Stem Cells after RNA Interference-Mediated Silencing of OCT4 and Nanog. *Stem Cells* **2006**.
6. Hyslop, L.; Stojkovic, M.; Armstrong, L.; Walter, T.; Stojkovic, P.; Przyborski, S.; Herbert, M.; Murdoch, A.; Strachan, T.; Lako, M. Downregulation of NANOG Induces Differentiation of Human Embryonic Stem Cells to Extraembryonic Lineages. *Stem Cells* **2005**.
7. Wang, Z.; Oron, E.; Nelson, B.; Razis, S.; Ivanova, N. Distinct lineage

specification roles for NANOG, OCT4, and SOX2 in human embryonic stem cells. *Cell Stem Cell* **2012**, *10*, 440–454.

8. Li, A.I.; Hokugo, A.; Jarrahy, R.; Zuk, P.A. Human adipose tissue as a source of multipotent stem cells. In *Stem Cells in Aesthetic Procedures: Art, Science, and Clinical Techniques*; 2014 ISBN 9783642452079.
9. Zuk, P.A.; Zhu, M.; Mizuno, H.; Huang, J.; Futrell, J.W.; Katz, A.J.; Benhaim, P.; Lorenz, H.P.; Hedrick, M.H. Multilineage cells from human adipose tissue: implications for cell-based therapies. *Tissue Eng.* **2001**.
10. Gronthos, S.; Franklin, D.M.; Leddy, H.A.; Robey, P.G.; Storms, R.W.; Gimble, J.M. Surface protein characterization of human adipose tissue-derived stromal cells. *J. Cell. Physiol.* **2001**.
11. Dominici, M.; Le Blanc, K.; Mueller, I.; Slaper-Cortenbach, I.; Marini, F.; Krause, D.; Deans, R.; Keating, A.; Prockop, D.; Horwitz, E. Minimal criteria for defining multipotent mesenchymal stromal cells. The International Society for Cellular Therapy position statement. *Cytotherapy* **2006**.
12. De Francesco, F.; Tirino, V.; Desiderio, V.; Ferraro, G.; D'Andrea, F.; Giuliano, M.; Libondi, G.; Pirozzi, G.; De Rosa, A.; Papaccio, G. Human CD34+/CD90+ ASCs are capable of growing as sphere clusters, producing high levels of VEGF and forming capillaries. *PLoS One* **2009**.
13. Pitrone, M.; Pizzolanti, G.; Tomasello, L.; Coppola, A.; Morini, L.; Pantuso, G.; Ficarella, R.; Guarnotta, V.; Perrini, S.; Giorgino, F.; et al. NANOG plays a hierarchical role in the transcription network regulating the pluripotency and plasticity of adipose tissue-derived stem cells. *Int. J. Mol. Sci.* **2017**, *18*, 1–16.
14. Potdar, P.D.; Sutar, J.P. Establishment and molecular characterization of mesenchymal stem cell lines derived from human visceral & subcutaneous adipose tissues. *J. Stem Cells Regen. Med.* **2010**.
15. Langroudi, L.; Forouzandeh, M.; Soleimani, M.; Atashi, A.; Golestaneh, A.F. Induction of differentiation by down-regulation of Nanog and Rex-1 in cord blood derived unrestricted somatic stem cells. *Mol. Biol. Rep.* **2013**, *40*, 4429–4437.
16. Perrini, S.; Ficarella, R.; Picardi, E.; Cignarelli, A.; Barbaro, M.; Nigro, P.; Peschechera, A.; Palumbo, O.; Carella, M.; De Fazio, M.; et al. Differences in Gene Expression and Cytokine Release Profiles Highlight the Heterogeneity of Distinct Subsets of Adipose Tissue-Derived Stem Cells in the Subcutaneous and Visceral Adipose Tissue in Humans. *PLoS One* **2013**.
17. Lengner, C.J.; Camargo, F.D.; Hochedlinger, K.; Welstead, G.G.; Zaidi, S.; Gokhale, S.; Scholer, H.R.; Tomilin, A.; Jaenisch, R. Oct4 Expression Is Not Required for Mouse Somatic Stem Cell Self-Renewal. *Cell Stem Cell* **2007**.
18. Rodeheffer, M.S.; Birsoy, K.; Friedman, J.M. Identification of White Adipocyte Progenitor Cells In Vivo. *Cell* **2008**.
19. Smas, C.M.; Sul, H.S. Pref-1, a protein containing EGF-like repeats, inhibits adipocyte differentiation. *Cell* **1993**.

20. Tang, W.; Zeve, D.; Suh, J.M.; Bosnakovski, D.; Kyba, M.; Hammer, R.E.; Tallquist, M.D.; Graff, J.M. White fat progenitor cells reside in the adipose vasculature. *Science (80-.).* **2008**.
21. Tseng, Y.H.; Butte, A.J.; Kokkotou, E.; Yechoor, V.K.; Taniguchi, C.M.; Kriauciunas, K.M.; Cypess, A.M.; Niinobe, M.; Yoshikawa, K.; Patti, M.E.; et al. Prediction of preadipocyte differentiation by gene expression reveals role of insulin receptor substrates and necdin. *Nat. Cell Biol.* **2005**.
22. Wang, Y.; Hudak, C.; Sul, H.S. Role of preadipocyte factor 1 in adipocyte differentiation. *Clin. Lipidol.* 2010.
23. Wang, Y.; Kim, K.-A.; Kim, J.-H.; Sul, H.S. Pref-1, a Preadipocyte Secreted Factor That Inhibits Adipogenesis. *J. Nutr.* **2018**.
24. Mitterberger, M.C.; Lechner, S.; Mattesich, M.; Kaiser, A.; Probst, D.; Wenger, N.; Pierer, G.; Zwerschke, W. DLK1(PREF1) is a negative regulator of adipogenesis in CD105+/CD90+/CD34+/CD31-/FABP4- adipose-derived stromal cells from subcutaneous abdominal fat pats of adult women. *Stem Cell Res.* **2012**, *9*, 35–48.
25. Biniszkiewicz, D.; Gribnau, J.; Ramsahoye, B.; Gaudet, F.; Eggan, K.; Humpherys, D.; Mastrangelo, M.-A.; Jun, Z.; Walter, J.; Jaenisch, R. Dnmt1 overexpression causes genomic hypermethylation, loss of imprinting, and embryonic lethality. *Mol. Cell. Biol.* **2002**.
26. Tsai, C.C.; Su, P.F.; Huang, Y.F.; Yew, T.L.; Hung, S.C. Oct4 and Nanog Directly Regulate Dnmt1 to Maintain Self-Renewal and Undifferentiated State in Mesenchymal Stem Cells. *Mol. Cell* **2012**.
27. Wade Harper, J.; Adami, G.R.; Wei, N.; Keyomarsi, K.; Elledge, S.J. The p21 Cdk-interacting protein Cip1 is a potent inhibitor of G1 cyclin-dependent kinases. *Cell* **1993**.
28. Xiong, Y.; Hannon, G.J.; Zhang, H.; Casso, D.; Kobayashi, R.; Beach, D. P21 is a universal inhibitor of cyclin kinases. *Nature* **1993**.
29. Aleem, E.; Kiyokawa, H.; Kaldis, P. Cdc2-cyclin E complexes regulate the G1/S phase transition. *Nat. Cell Biol.* **2005**.
30. Gartel, A.L.; Tyner, A.L. Transcriptional regulation of the p21((WAF1/CIP1)) gene. *Exp. Cell Res.* **1999**.
31. Fouse, S.D.; Shen, Y.; Pellegrini, M.; Cole, S.; Meissner, A.; Van Neste, L.; Jaenisch, R.; Fan, G. Promoter CpG Methylation Contributes to ES Cell Gene Regulation in Parallel with Oct4/Nanog, PcG Complex, and Histone H3 K4/K27 Trimethylation. *Cell Stem Cell* **2008**.
32. Lei, H.; Oh, S.P.; Okano, M.; Jüttermann, R.; Goss, K.A.; Jaenisch, R.; Li, E. De novo DNA cytosine methyltransferase activities in mouse embryonic stem cells. *Development* **1996**.
33. Okano, M.; Bell, D.W.; Haber, D.A.; Li, E. DNA methyltransferases Dnmt3a and Dnmt3b are essential for de novo methylation and mammalian development. *Cell* **1999**.
34. Coppola, A.; Tomasello, L.; Pitrone, M.; Cillino, S.; Richiusa, P.; Pizzolanti, G.;

Giordano, C. Human limbal fibroblast-like stem cells induce immune-tolerance in autoreactive T lymphocytes from female patients with Hashimoto's thyroiditis. *Stem Cell Res. Ther.* **2017**.

35. Tomasello, L.; Mauceri, R.; Coppola, A.; Pitrone, M.; Pizzo, G.; Campisi, G.; Pizzolanti, G.; Giordano, C. Mesenchymal stem cells derived from inflamed dental pulpal and gingival tissue: A potential application for bone formation. *Stem Cell Res. Ther.* **2017**.
36. Riccardi, C.; Nicoletti, I. Analysis of apoptosis by propidium iodide staining and flow cytometry. *Nat. Protoc.* **2006**.